Document downloaded from:

http://hdl.handle.net/10251/195072

This paper must be cited as:

Serrano, J.; Climent, H.; Piqueras, P.; Darbhamalla, A. (2022). Energy recovery potential by replacing the exhaust gases recirculation valve with an additional turbocharger in a heavy-duty engine. Energy Conversion and Management. 271:1-11. https://doi.org/10.1016/j.enconman.2022.116307

The final publication is available at

https://doi.org/10.1016/j.enconman.2022.116307

Copyright Elsevier

Additional Information

Energy recovery potential by replacing the exhaust gases recirculation valve with an additional turbocharger in a heavy-duty engine

José Ramon Serrano, Héctor Climent*, Pedro Piqueras, Aditya Darbhamalla

CMT Motores Térmicos, Universitat Politècnica de València, Spain

*Corresponding author: hcliment@mot.upv.es. Telephone: (+34) 96 387 76 50. Postal address: CMT Motores Térmicos. Universitat Politècnica de València. Camino de Vera s/n. 46022. Valencia. Spain.

Highlights

- Replacement of EGR valve with a second set of turbochargers for energy recovery
- Analysis of different twin-turbocharging architectures in HD engine
- Comparison of results with experimental data for validating the EGR and fuel benefits
- Twin turbocharging increases EGR and benefits in fuel consumption up to 5% and 7% respectively

Key Words: Energy recovery, fuel economy, heavy-duty CI engine, Twin Turbocharging, EGR system.

Abstract

A simulation-based study is performed to assess different twin-turbocharging configurations, used to allow energy recovery from exhaust gas recirculation, over single-stage turbocharging architecture. The baseline configuration is a single-stage turbocharged engine equipped with a low-pressure exhaust gas recirculation ~~(LP-EGR)~~ system. Experimental data from an engine test bench is used to calibrate this turbocharging architecture model. The novelty ~~objective~~ of this study is to evaluate the energy recovery potential by replacing the low-pressure exhaust gas recirculation ~~LP-EGR~~ valve with a turbine so that the flow energy is not lost during the expansion of the valve. This additional turbine is coupled to a compressor placed in the intake line so that the turbocharging system in the heavy-duty compression ignition engine is converted into a twin-turbocharging architecture. Different turbocharging configurations are tested to attain maximum EGR rates at 1100, 1500, and 2200 RPM engine speeds with boosting pressures ranging from 1.8 to 2.6 bar. Fuel consumption calculations have been performed at constant EGR rates for all three speeds and 1500 RPM partial load operation. It is concluded that twin-turbocharging has benefits to attaining about 5% more EGR rates and saves up to 7% in fuel economy when compared with single-stage turbocharging.

1 Introduction

The exhaust Gases Recirculation (EGR) technique is widely used to reduce NOx emissions in an internal combustion engine. By implementing EGR the combustion temperature is reduced and thereby NOx formation. Exhaust gases can be circulated in two ways: High-Pressure EGR (HPEGR) loop/short route and the Low-Pressure EGR loop (LPEGR)/long route. The delivery of the exhaust gases is routed using EGR valves or waste gates used in LPEGR and HPEGR respectively. Several researchers have investigated the advantages and disadvantages of such systems. The researchers from [1] have demonstrated results comparing four different EGR loops (2 in each LP and HP EGR loop) and concluded that the LP EGR loop provides better brake-specific fuel consumption (BSFC). Authors in [2] have analyzed the fuel penalty that occurred due to the usage of the HP-EGR loop

because of the high pumping losses over the LPEGR loop. CFD simulation studies have been performed to understand the improvements that can be achieved using HP EGR per cylinder using advanced diesel fuel [3]. From the same, it was also concluded that using both the EGR loops, low emissions can be attained up to partial loads. Results from [4] show that a proper matching of VGT control is required to attain the advantages of the HP-EGR loop to reduce pumping loss and attain better BSFC. The same has also been concluded by [5] using a different approach by regulating exhaust gases in a short route EGR loop using an EGR valve.

It is also true that using high EGR rates influences the fuel economy and increases PM/soot emissions due to lack of oxygen. To overcome the above problem several researchers have implemented dual turbocharging to increase boost pressure, hence, increasing fresh charge. Dual-stage turbocharging is a technique where the compressor and turbine function in series. Also, dual-stage turbochargers use a wastegate to regulate back pressure and thereby the effect on fuel penalty. Using a dual-stage turbocharging configuration in a heavy-duty engine, CFD and experimental data have shown improvements in increased fresh charge and reduced PM emissions [6]. A trade-off between fuel consumption in LP and HP EGR loops is assessed while comparing the results of single and two-stage turbocharging [7]. Assessment of pumping loss is studied in [8] for a two-stage turbocharger which improved the breathing capability of the engine. Several turbo configurations were analyzed in steady ~~and transient engine operation~~ to understand the thermo-mechanical limitations of boosting architectures in steady-state [9] and transient engine running conditions [10]. Improvements in BSFC have been observed by adjusting compression ratio and intake valve lift in [11], to reduced pumping losses. Usage of dual-stage turbocharging is also assessed in gasoline partially premixed combustion under LP and HP EGR routes and results conclude high loads favor mixed route EGR loops while low loads favor LPEGR route[12]. Dual-stage turbocharging with bypass valves are used to test the effect of engine performance at different altitudes and has shown almost 8% improvement in dual-stage turbocharging at lower altitudes[13]. Improved power density and efficiency of the marine engine using two stage turbocharger are studied for lower exhaust energy loss [14]. Advanced neural networks for nonlinear predictive control strategy for two-stage turbochargers are studied for accuracy in comparison with PID control and results of high accuracy are shown[15].

Homogeneous Charge Compression Ignition (HCCI) is a form of internal combustion in which well-mixed fuel and air are compressed to the point of auto-ignition. In HCCI combustion improvements in combustion efficiency are observed at low loads while using LP-EGR. An HP-EGR loop is also necessary, as concluded in [16], to experience overall improvements to reduce emissions. Premixed dual fuel used in DI HCCI engines has shown improvements in emissions at low fuel temperature, as temperature increases lead to higher NOx emissions as studied by [17]. In a single-cylinder DI engine, injection timing is controlled and results show that PM and NOx emissions can be regulated with high EGR rates [18]. Research on EGR is extended to RCCI engines as well, where EGR is used to regulate the in-cylinder pressure, and fuel economy and extend maximum loads with lower emissions[19]. HPEGR along with biodiesel is used in RCCI engines and results have shown decrement in NOx but have an impact on fuel economy, CO, and HC emissions as depicted in [20].

As the exhaust gas percentage in the intake manifold increases, the fresh charge intake temperature also increases. To reduce the charge temperature along with high EGR rates several researchers have implemented dual fuels blended with natural gas or ethanol. This resulted in low combustion

temperature and low exhaust gas temperature, as discussed in [21], [22]. pre-chamber combustion using dual-fuel such as methane and diesel in HD engines is tested for lower emissions and has proved to be a reduction in NOx production by up to 50% [23]. Others have implemented EGR coolers to regulate the temperature of exhaust gases or have imposed premixing of both the exhaust gases and fresh charge and using charge coolers to see added benefits in emissions and BSFC as shown in [19],[20],[21].

In addition, dual-stage turbocharging has always been in prime focus to improve boost pressure and observe improvements in both BSFC and emissions. Effects on imposing high boost pressure using ultra backward curved impeller compressors, along with the use of aerodynamic cabins have provided improved fuel consumption in heavy-duty engines as proposed by [27]. The effects of dual-stage turbocharging for better fuel economy and emissions are shown in [23],[24],[25]. Research has also shown the usage of the Stirling engine to recover energy from exhaust gases in an HD engine and has shown marginal improvements in fuel consumption and significant improvement in power output[31]. The effect of back pressure on engine performance due to poor design is analyzed and presented in [32]. Turbo matching at elevated back pressure in marine engines is studied to optimize engine performance[33]. Under the same condition of higher exhaust gas pressure, a mini-review on waste gate analyses has been performed for EGR to reduce emissions is studied in[34].

Exhaust gas energy is not only recovered using dual or two-stage turbocharging but also using the miller cycle or Organic Rankine cycle (ORC) is also used. Results on the usage of ORC are studied for tradeoffs in backpressure, space, weight, and thermal efficiency [35]. Usage of the miller cycle is studied over a two-stage boosting technique and results of lower filling losses and higher power density are presented in [36]. A detailed analysis of different heat recovery modes is studied using a thermoelectric generator, heat pipes, ORC, and Solar Rankine cycle (SRC), and the results of efficiency improvement of an engine are studied in[37]. Limitations on heat recovery using the thermoelectric generator and heat pipes due to low efficiency and high heat transfer respectively are presented by [38]. Results on enhanced performance of heat pipes over thermoelectric motor are studied and presented with more than 43% increase in power is presented [39]. Back pressure limitation because of usage of the thermoelectric generator is presented in [40]. Simultaneous power generation and heat recovery using a heat pipe-assisted thermoelectric generator system are theoretically studied and the results are presented in [41].

The novelty of this work lies in the replacement of the EGR valve with a second set of turbochargers. (I)This includes the elimination of the usage of any kind of EGR valve/back pressure valve or waste gate. (II)In the twin-turbocharging configuration, the turbine configurations are always working parallel. (III)And based on the functionality of compressors the configurations are classified as parallel or series architecture. (IV) results are compared for back pressure, fuel consumption rate, and maximum EGR rates. For the current study different types of twin-turbocharging architectures are assessed to avoid the flow energy loss happening in the EGR valve to control the exhaust gas's mass flow to the intake system. Since EGR rates are increasingly higher to handle NOx emissions, using a turbine instead of an EGR valve leads to recovering exhaust gas energy to move a second turbocharger. A model-based evaluation of several dual-stage architectures is given in this paper to attain high EGR rates and improved BSFC compared to the baseline engine with a single-stage turbocharger equipped with an EGR valve. A detailed description of the procedure is provided in the

methodology section. The tools and modeling details are described in section 3. Results from the simulation study are presented and discussed. Finally, the conclusions showing the main outcomes of this study are given in the last section.

2 Methods

A validated engine model is used as the base configuration [42] and a few results of the validation are presented in section.4. This model is developed using a 1D code in the GT-Power software stack. A four-stroke, six-cylinder, direct injection, and turbocharged heavy-duty diesel engine is used. The turbocharger used for this application is a map-based model. The engine model is equipped with a low-pressure EGR system, which includes an EGR valve to attain the desired EGR rates. A schematic layout is shown in Fig. 1.

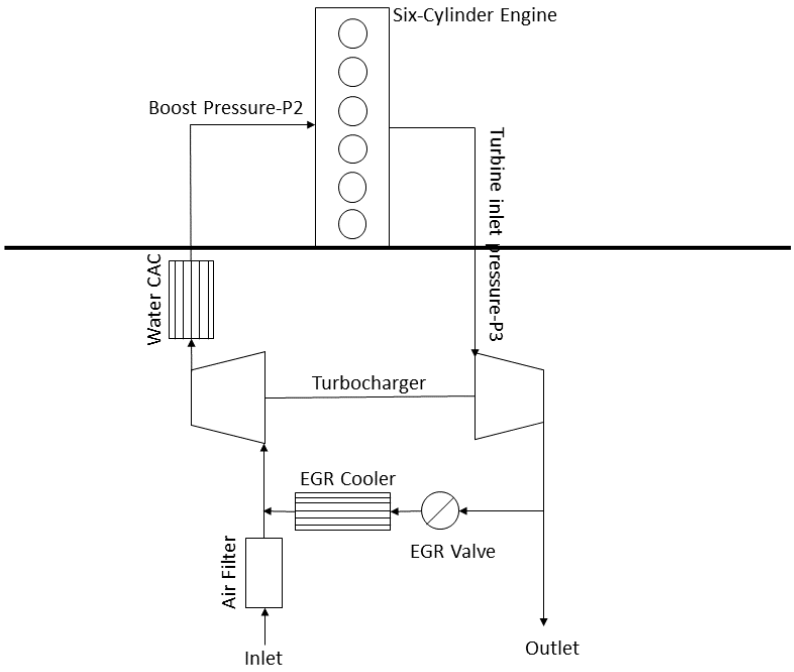

1

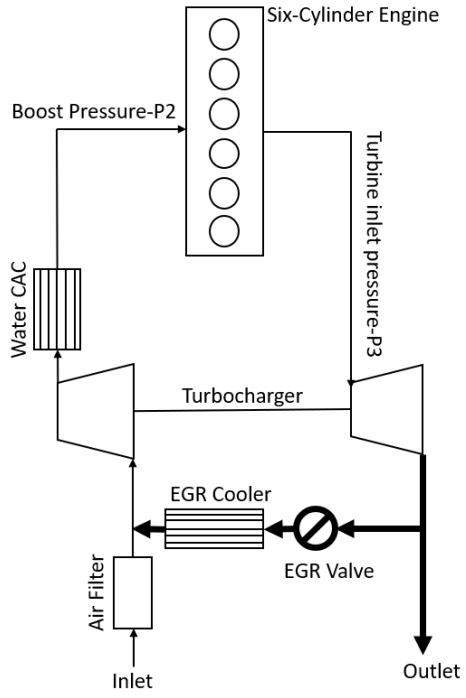

2

3 Figure 1:Schematic layout of the baseline configuration

4 In this study, the EGR valve is replaced with another turbocharger for assessing twin-turbocharging
5 architectures. Therefore, both turbines are always working in parallel and, based on their
6 compressors' operation layout, the architectures are classified as parallel and series configurations.
7 In a parallel configuration, as depicted in picture A, in Fig. 2, both compressors work to attain similar

inlet manifold pressure. Based on the size of the compressor, the inlet charge (Air+EGR) splits into individual compressor inlet flows. In series configuration, the boost pressure is attained in stages. The air charge is pressurized from nearly ambient conditions to an intermediate pressure (P2') and from P2' to actual intake manifold pressure. Based on the addition of EGR, series architecture is classified as series-1, 2, and 3. In the series-1 configuration, as shown in picture B in Fig. 2, the EGR mass flow is added directly into the intake manifold. While in series-2 architecture, as observed in picture C in Fig. 2, the addition of exhaust gases takes place at the intermediate stage of compression, i.e., at P2'. Whereas in series-3, represented schematically in picture D in Fig. 2, the EGR is supplied to the system upstream of the stage-1 compressor.

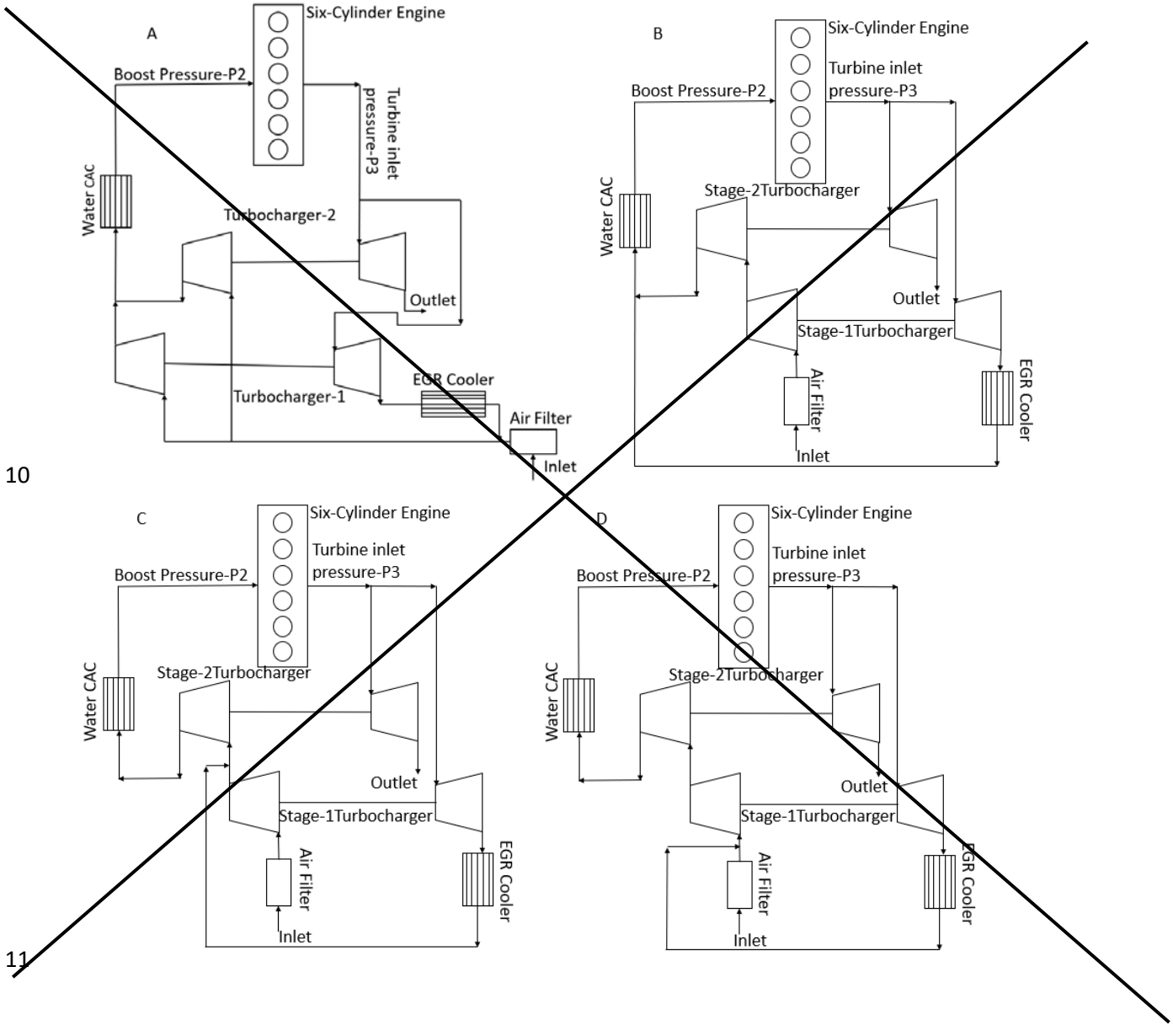

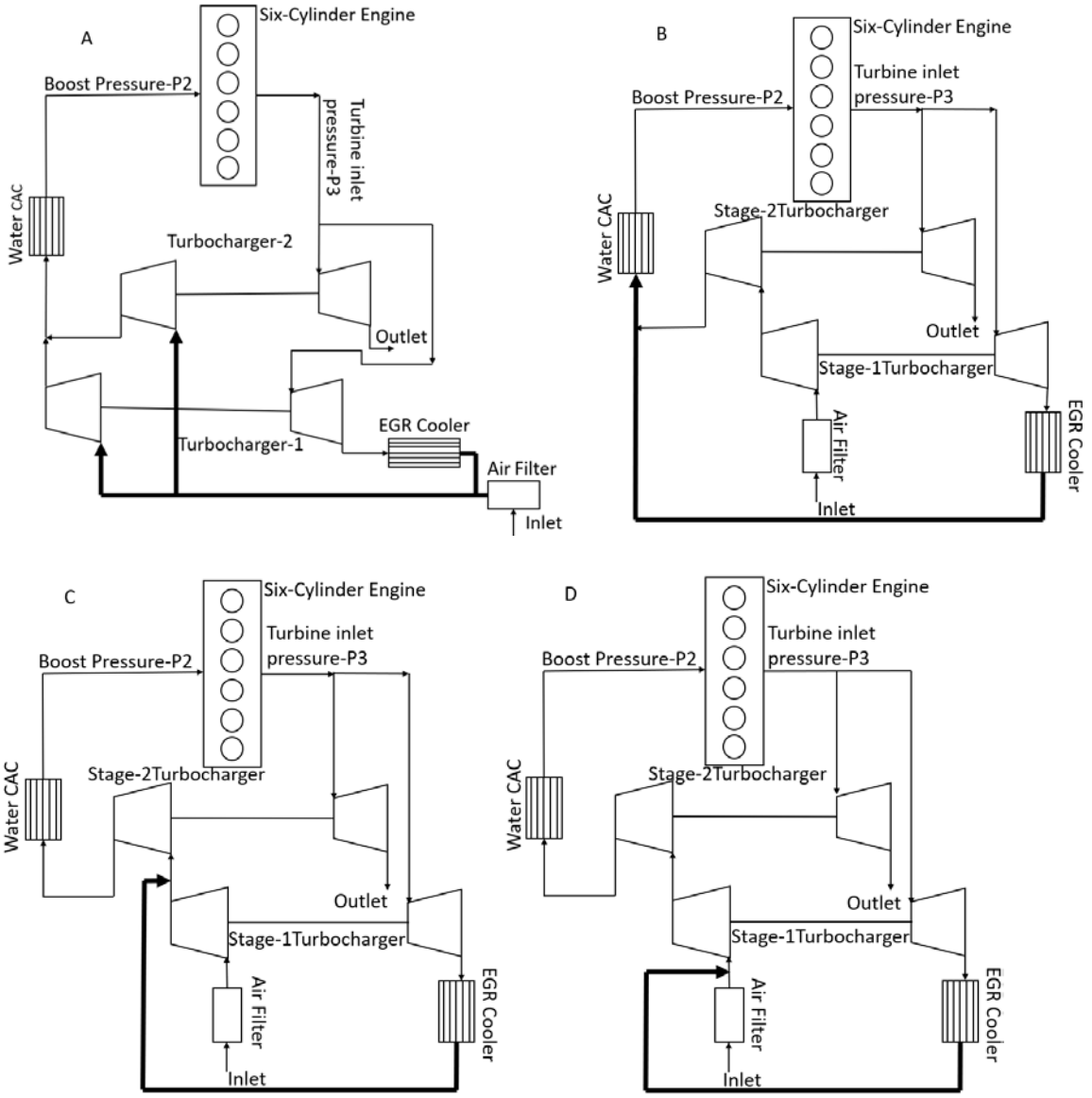

Figure 2: Schematic layout of Twin turbocharging, Parallel (A), Series-1 (B), Series-2 (C), and Series-3 (D)

To assess the main objective of the study, simulations are performed at 1100, 1500, and 2200 RPM. The air-to-fuel ratio (AFR) is maintained at 18, to account for lean combustion. The peak pressure inside the cylinder is restricted to a maximum of 220 bar, typical for heavy-duty engines. All turbocharger configurations are tested for the same boost pressure, ranging from 1.8 to 2.6 bar. Thermo-mechanical limitations were considered for the pressure at the inlet of the turbines (P3), not to exceed 4.5 bar in average value. For this analysis, the pressure and temperature conditions in the intake manifold were the same throughout all the configurations.

In both single and twin-turbocharging configurations, mass flow multipliers applied to the original engine compressor and turbine maps were used to adjust the size of the turbocharger. These were modified to attain a 70% compressor efficiency and a 60% turbine efficiency. In the base

configuration, a constant mass flow multiplier of 0.7 is employed in the turbine to attain the desired boost pressure and efficiency. Firstly, a feasibility analysis is performed on all the configurations for the above-described limits, and failed models are discarded from any further analysis. Then the turbochargers configurations are assessed to attain maximum EGR rates at all the mentioned speeds and loads. Architectures are also assessed for fuel consumption by evaluating the Brake Specific Fuel Consumption (BSFC). BSFC is analyzed under two different conditions, one at a constant EGR rate at all engine speeds and the other at 1500 RPM to attain 700 Nm torque, which is the partial load study.

Finally, from the above analyses, architecture attaining higher EGR, and lower fuel consumption rates is used for comparison with experimental results. The experiments are conducted at different speeds, boost pressure, and loads using a single-stage turbocharger with an LP-EGR loop, and EGR mass flow is regulated using an EGR valve. The simulation-based assessment was conducted using the above experimental results to compare single-stage turbocharging (base configuration) and twin-turbocharging (Series-2 architecture) for EGR rates and BSFC. In this study for a fair comparison, the stage-2 turbocharger in twin-turbocharging is equipped with the same sized compressor and turbine as that of the main turbocharger in the base configuration. And for the stage-1 turbocharger, the size of the compressor and turbine are maintained constant throughout this assessment.

3 Tools and model description

As mentioned earlier, the GT power software stack was employed to develop the 1-D model. The model is equipped with pipes, bends, flow splitters, Water Charged Air Cooler (WCAC), an EGR cooler, and a turbocharger. The discretization of the intake and exhaust manifolds is modeled to analyze pressure, temperature, and mass flow rates at desired locations.

To regulate the temperature in the intake manifold, all the configurations employed a WCAC. And to cool the exhaust gases an EGR cooler has been used. Ideal efficiencies for the WCAC and EGR cooler were employed by maintaining the water temperature at 298 K in WCAC and 350 K for coolant in the EGR cooler. The pressure loss across the EGR cooler is calibrated by using experimental data as mentioned in [43]. The pressure loss in the intake and exhaust manifolds is validated using experimental data in the baseline configuration. A similar pressure drop is considered for twin-turbo charging configurations.

The information related to the turbocharger comes from the characteristic maps measured in the turbocharger test bench [42]. Fig. 3 shows the information on the compressor and turbine maps. These data correspond to a particular compressor and turbine that can be adjusted for each application to achieve particular objectives. The information depicted in Fig.3(A), corresponds to the compressor map. The solid black line represents iso speed lines from the lowest RPM of 50 KRPM to 150KRPM. The dotted black lines represent iso efficiency lines, efficiencies ranging from 50% efficiency to 75% efficiency on average. The surge limit is plotted as a red solid line, operating point beyond this limit leads to poor performance of the turbocharger and thereby the engine. Using eqn.1, the corrected mass flow rate is obtained and plotted against the pressure ratio. In Eq. (1) T_{in} and P_{in} are the compressor static inlet Temperature and Pressure. While T_{ref} and P_{ref} are the reference pressure and temperature, which are 1 bar and 273 K. The information depicted in Fig.3(B) is for the turbine map, Plotted for different VGT positions and reduced mass flow and speeds using

Eq. (2) and (3). To attain the objectives for the current analysis mass flow multipliers are employed. Optimizing the compressor efficiency throughout most engine running conditions, which usually means the operation of the compressor near surge for low engine speeds and high engine loads, and near over speed limit at high engine speeds and high engine loads. The turbine consists of a variable geometry turbine (VGT), which controls the pressure in the intake manifold. Hence, VGT operation involves the closest guide vane for achieving high boost pressures and wide-open positions would lead to low values of intake manifold pressure.

$$\dot{m}_{corrected} = \dot{m}\sqrt{\frac{T_{in}}{T_{ref}}}\frac{p_{ref}}{p_{in}} \quad (1)$$

$$\dot{m}_{reduced} = \frac{\dot{m}\sqrt{T_{in}}}{p_{in}} \quad (2)$$

$$N_{reduced} = \frac{N}{\sqrt{T_{in}}} \quad (3)$$

Concerning engine control, a VGT turbocharger is employed in the base configuration. This device controls the boost pressure in the inlet manifold. For this application, a PID controller is employed and tuned for stability. The EGR valve is controlled using another PID, adjusting the throttle angle for desired mass flow rates of exhaust gases. In twin-turbocharging, both turbochargers are equipped with similar turbocharger maps. Stage-2 turbocharger is equipped with a VGT, which controls the intake manifold pressure using a tuned PID controller. On the other hand, the stage-1 turbocharger regulates the EGR mass flow. Firstly, the size of the turbine is adjusted to attain the desired turbine efficiency and then the rack position is altered for attaining maximum exhaust gases without losing efficiency.

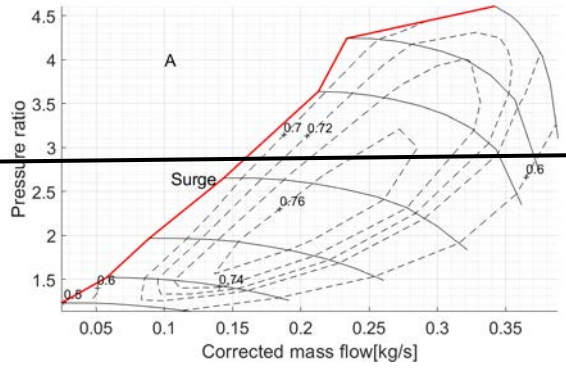
A
Surge
Pressure ratio
Corrected mass flow[kg/s]
0.7
0.72
0.6
0.76
0.74
0.6
0.6

1

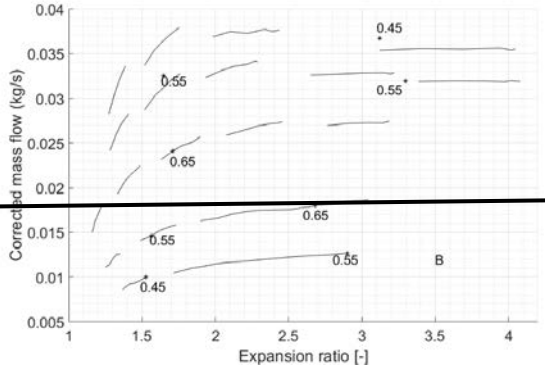
Corrected mass flow (kg/s)
Expansion ratio [-]
0.45
0.55
0.55
0.65
0.65
0.55
0.55
0.45
B

2

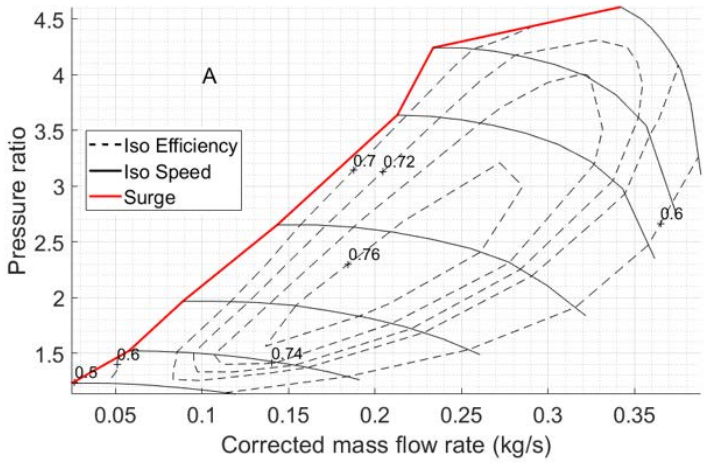
A
Iso Efficiency
Iso Speed
Surge
Pressure ratio
Corrected mass flow rate (kg/s)
0.7
0.72
0.6
0.76
0.74
0.6
0.6

3

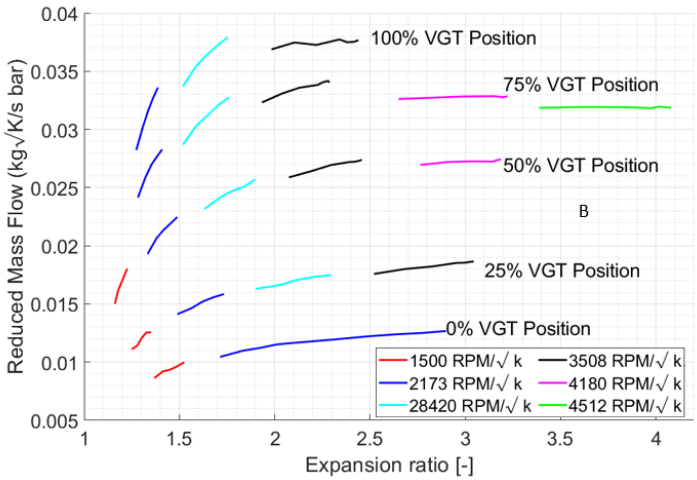

Figure 3: A: Compressor Map, B: Turbine Map

4 Model Validation

For the model validation, experimental results at low speed/low load and high speed/full load data are used. Since the study focuses on energy recovery through EGR, instantaneous pressure traces are assessed for both intake manifold pressure and pressure of the exhaust gases. Fig.4 depicts the information on the pressure traces for the same plotted against CAD(°). In both plots in Fig.4, it can be observed that the model predicts the experimental results with a close proximity, with an absolute maximum deviation of 4%. These results confirm the stability of the fluid dynamic properties of the model. To show the thermal stability of the model prediction, information on the average temperature data is used for both intake manifold and exhaust gas temperature. The data is shown in table.1, it also depicts the information on the average mass flow rate of air and EGR. It can be observed from the table.1 that the average absolute deviation in temperature is about 5°C. Also, from the same, it can be observed that the mass flow rate deviation is about 3% observed at full load conditions. While the error in prediction of the model to experimental data at low load conditions is almost negligible.

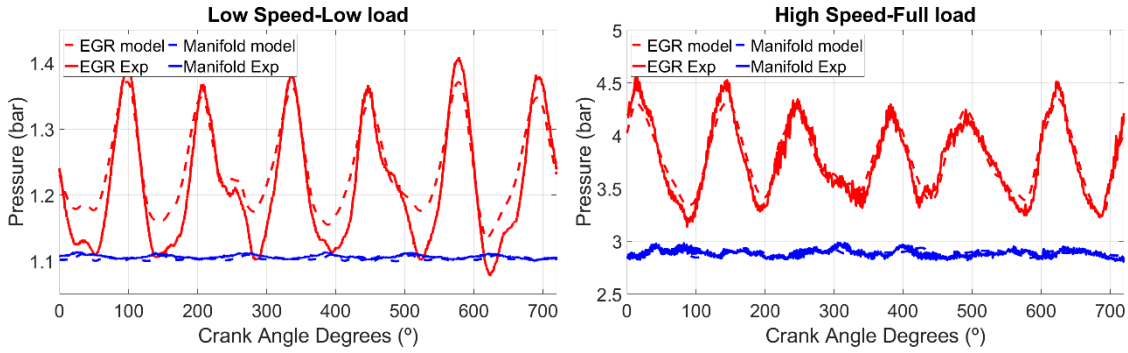

Figure 4: Instantaneous Pressure traces of EGR and intake Manifold at low speed/low load and high speed/full load

Table 1: Model to Experimental comparison of mass flow rates and temperature

Speed/Load	Air Mass flow (g/s)		EGR mass flow (g/s)		Temperature manifold (°C)		Temperature EGR(°C)	
	Exp.	Model	Exp.	Model	Exp.	Model	Exp.	Model
Low/Low	60.5	60.5	13.5	13.5	34.4	32.7	55.6	68.1
High/Full	343.8	334.2	28.8	28.8	62.6	61.8	89.4	92.7

Observing the instantaneous pressure traces, averaged mass flow rate and temperature results show the model is thermo-fluid dynamically stable to a satisfactory level and therefore the model can be used for future assessment.

5 Results and Discussions

Initial investigation of the turbo configuration showed that series-1 and series-3 have issues attaining the previously mentioned standards of functionality. Therefore, a feasibility analysis is performed.

5.1 Compatible solutions analysis

In series-1 configuration Fig.2(B), exhaust gases are added directly into the intake manifold before WCAC. This layout has caused severe fluctuations in pressure across the stage-1 turbine (EGR Turbine). The cause of these pulsations is due to the high boost pressure employed in this study leading to reverse flow. Instantaneous pressures are analyzed upstream and downstream of the turbine and plotted against the crank angle degree as shown in Fig. 5. From the results plotted in Fig. 5, it is observed that the pressure at the outlet of the turbine is higher than that of at the inlet of the turbine. ~~For instance, in Fig.4 for CAD 0-50, as the pressure difference between the pressure upstream the turbine (inlet) to pressure downstream the turbine (outlet) is high, there is no mass flow rate through the turbine~~ .The flow of energy always takes places from high pressure zone to low pressure. And as GT-power is obliged to follow the laws of conversion of energy, this contradicting phenomena has led to no mass flow rate passing through the turbine. In certain phases of the engine cycle, the simulation provides inconsistent turbine operation which leads to the conclusion that given typical turbine and compressor efficiencies employed in HD engines, placing a turbine between the exhaust and intake manifolds as done in series-1 configuration is dysfunctional.

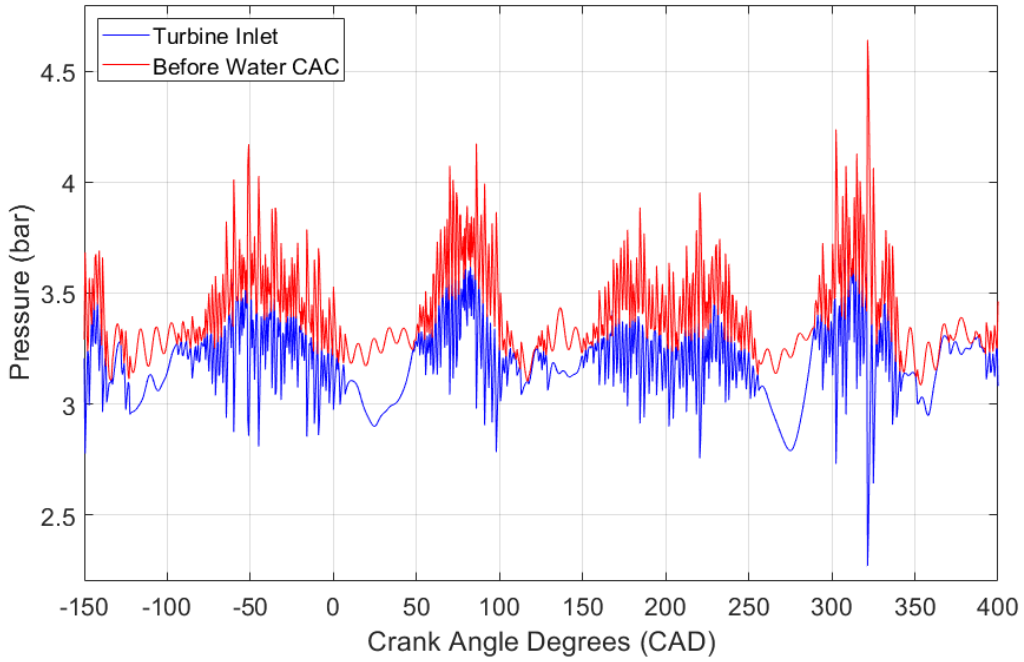

Figure 5:CAD vs Pressure for Series-3 configuration

In the series-3 configuration, exhaust gases are added along with the fresh charge upstream of the stage-1 compressor. To accommodate all the charges, the compressor size must be increased. Due to an increase in the compressor size, the power consumption of the compressor increases, which will influence the pressure ratio. To maintain the desired boost pressure the turbine size must be reduced. This mismatch in the sizes of the turbine and compressor fails to attain high efficiencies.

An analysis conducted on the mass flow rates, as shown in Fig. 5, describes the above phenomena. In all the configurations the total mass flow rates are the same. In parallel configuration, the mass flow splits downstream the compressors based on the size of the compressor and the power from the turbine. Then, downstream of the compressors, they sum up the total mass flow rate in the intake manifold. In series-2 architecture, the stage1 compressor, compresses the fresh air from ambient pressure to P2´and at this location the exhaust gases are added, approximately 0.06 kg/s, making the total charge of mass flow at the inlet of stage-2 compressor equal to the total required mass flow. While in series-3 configuration, all the charge is supplied at the inlet of the compressor, therefore it is necessary to have a higher compressor size, which fails to meet the standards.

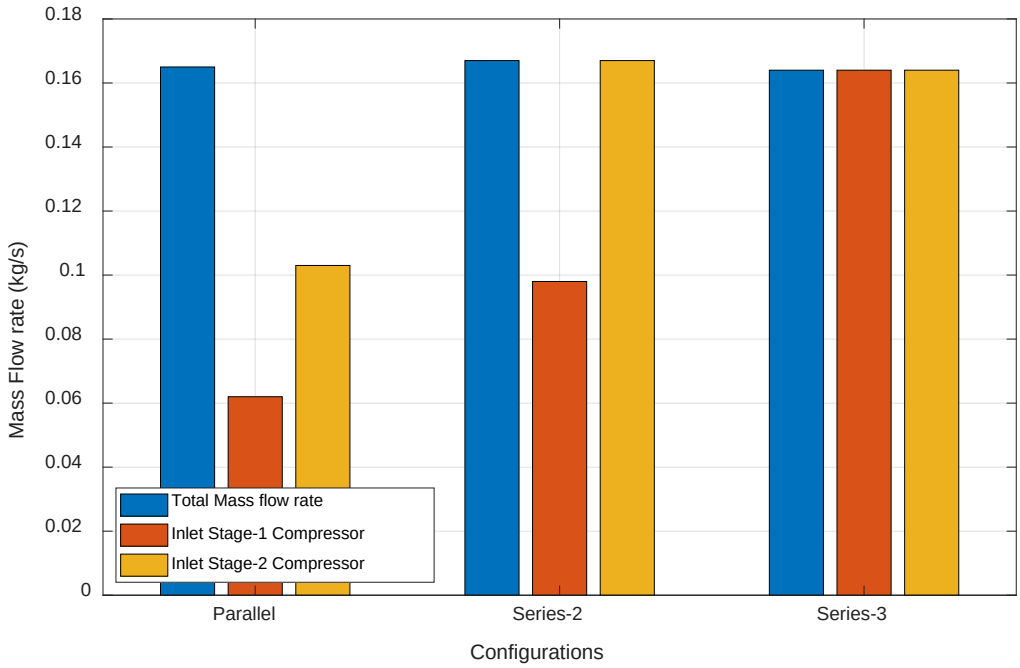

Figure 6: Mass flow rate analysis at each compressor inlet

Due to the failure of Series-1 and 3 configurations, both architectures are discarded, and no further assessments are conducted for this study. Therefore, the remaining configurations (base, parallel, and series-2 architectures) are further assessed. Series-2 architecture is referred to as series configuration/architecture from now on.

5.2 Maximum EGR Study

Three different engine speeds are chosen to evaluate the maximum EGR rate potential of each turbocharging configuration. Fig. 7 shows the results of this study, where a total of 45 simulations (3 engine speeds, 3 turbocharging layouts, and 5 intake manifold pressure) are presented. The results depicted in Fig.7 (A),(C)&(E) provide the information on the maximum EGR (%) that can be attained at each engine speed plotted against boost pressure. The data provided in Fig.7 (B),(D)&(F) are for respective BMEP plotted against boost pressure. Different colors represent different turbocharger configurations. Solid red depicts information for the base configuration which is a single-stage turbocharger. A solid blue line shows the information on series architecture while solid green is for parallel configuration. ~~The data is plotted against boost pressure and the engine BMEP is given by the symbol color following the scale in the color bar~~. For base configuration, at all engine speeds the maximum EGR percentage is restricted to 50%. This is because the EGR valve is working at its limits i.e., full open condition. And therefore, at a constant AFR of 18 with an increase in boost pressure, an increase in the BMEP can be observed. This is because as the boost pressure increases the fresh charge of air also increases.

At 1100 RPM, both the twin turbochargers attain lower EGR rates compared to the base configuration. This is because the engine operation is at low speeds and the operation of the VGT is at its closest guide vane due to turbo-matching. To attain higher boost pressure at 1100 RPM, mean

a further closer of the VGT position. This would lead to a higher exhaust manifold pressure and have an impact on the turbine efficiencies. To attain 60% efficiency for the turbine and targeted boost pressure, higher mass flow rates of exhaust gases are passed through the VGT turbine to operate at a much open guide vane position. This resulted in lower mass flow rates of EGR and an increase in BMEP as boost pressure increased. Also, for the same operating condition lower exhaust pressures are observed for twin-turbocharging architectures when compared to base configuration. Trends on lower exhaust pressure of approximately 1 bar in average can be seen at 1100 RPM ~~can be seen in~~ plot A of Fig. 8.

~~As engine speed increases higher mass flows of fresh charge can be attained, leading to higher EGR rates. At 1500 RPM, the parallel configuration attains EGR percentages higher than the base and series architectures. But gradually decreases as boost pressure increases (Fig. 6-plot C). This is because of the increase in the exhaust manifold pressure, as the VGT rack position closes to attain the required boost pressure, back pressure increases. To maintain the exhaust pressure below the thermo-mechanical limit, EGR rates had to be regulated. Although, this has not resulted in higher BMEP as the exhaust pressure in the manifold is still high. Fig. 7-plot B shows the trends in the exhaust pressure. Similar trends can be seen at 2200 RPM for both EGR rates and BMEP in Fig. 6-plot C and exhaust manifold pressure- in Fig. 7-plot C, for the same reason.~~

Parallel Configuration: As engine speed increases higher mass flows of fresh charge can be attained, leading to higher EGR rates. In 1500 RPM, trends of decreasing EGR rates are observed with an increase in boost pressure from Fig.7(C). A maximum EGR rate of 58% is observed at low boost pressure and a 53% EGR rate is observed at highest boost pressure. The decline of the EGR rate is because of two reasons, on one hand, to attain a constant turbine efficiency of 60% and on the other hand to maintain the operating point below the thermo-mechanical limit of 4.5 bar in exhaust pressure. Therefore, a decrease in EGR trends can be observed with an increase in boost pressure from Fig.7(C). Attaining a higher EGR rate at low boost pressure led to low BMEP of approximately 11 bar in comparison to the base configuration where 14 bar BMEP is observed. A constant decrease in the EGR rate from low boost pressure to high boost pressure led to an increase in BMEP. Trends in increasing BMEP can be observed in Fig.7(D). with a maximum BMEP of approximately 18 bars for both base and parallel configuration. This is because of attaining almost similar EGR rates of 50-53%. Although, the decrease in EGR rate has benefited turbine efficiency, but has no improvement in exhaust manifold pressure leading to a lower BMEP in parallel configuration Fig.7(B). This is because of employing a ~~the~~ lower-size turbine ~~employed~~ in this study to attain 60% in turbine efficiency. Similar trends can be seen at 2200 RPM for both EGR rates and BMEP in Fig.7 (C) and (D) and exhaust manifold pressure- Fig. 8(C), for the same reason.

Series Configuration: Increasing EGR rates are observed with an increase in boost pressure and engine speed. Trends in increasing EGR rates can be seen in Fig.7(C) and (E) for respective engine speeds of 1500 and 2200 RPM . The trends in increasing EGR rates from 45% to approximately 55% can be seen at 1500 RPM. While an increase in EGR rate from 50% to 53% at 2200 RPM can be seen with increase in boost pressure. This increase in EGR rates has a minimal effect on the BMEP of the engine. This is because of the moderate size of the turbocharger employed in this configuration. This resulted in increased breathing capability of the engine resulting in lower exhaust pressure. Trends in lower exhaust manifold pressure can be seen in Fig.8, with approximately 1.5 bar lower back pressure in average. Higher BMEP, moderately high EGR rates, and lower exhaust pressure can

be seen with series configuration due to the employment of a moderate-sized turbocharger when compared to parallel and base configuration.

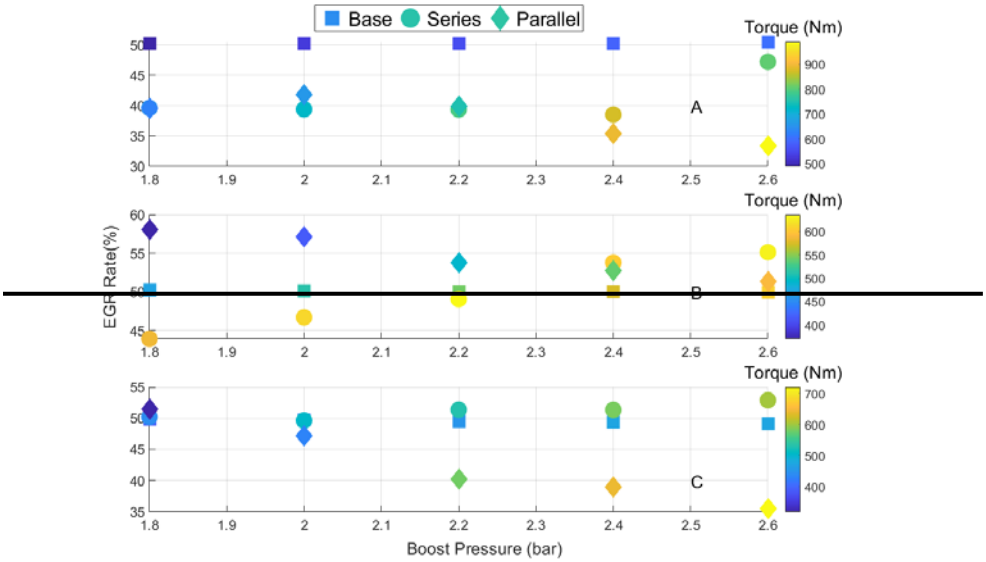

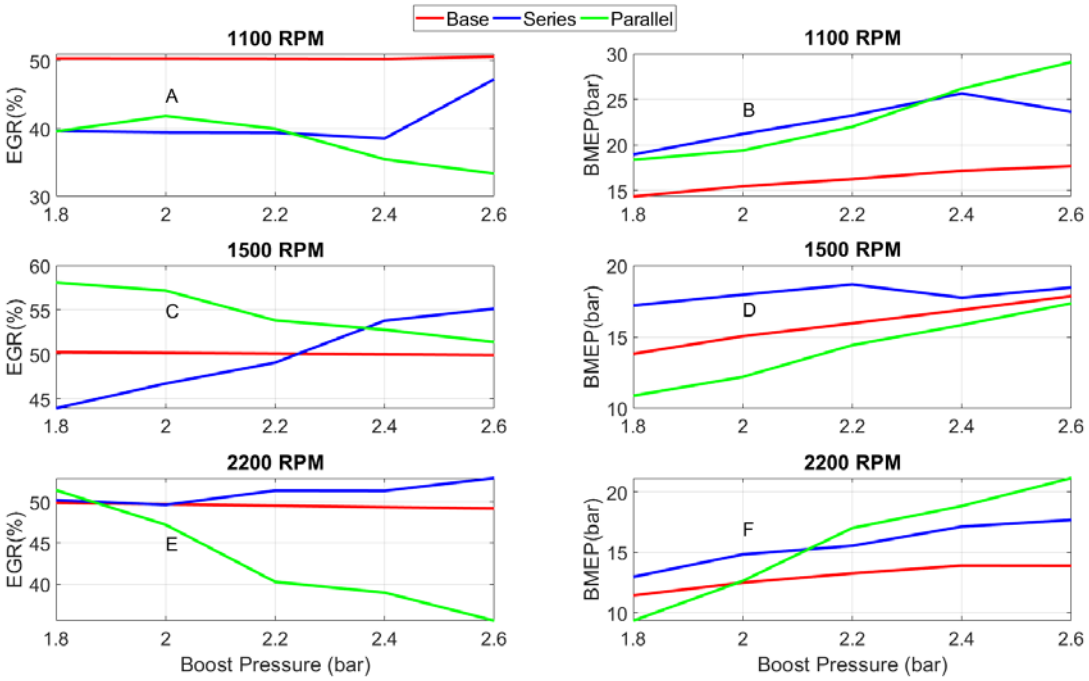

Figure 7: Boost pressure (bar) vs EGR(%) A:1100 RPM;C:1500 RPM;E:2200 RPM; Boost pressure (bar) vs BMEP(bar) B:1100 RPM;D:1500 RPM;F:2200 RPM.

Preliminary observation: Due to turbochargers matching to attain turbine efficiencies of 60%, the size of the turbocharger in parallel configuration has to be maintained small in comparison with series configuration. As the turbine size decreases, pressure at the inlet of the turbine increases having an impact on the BMEP and EGR rate. For this reason, engine performance to attain higher EGR rates decline with an increase in engine speed and boost pressure in a parallel configuration.

As the turbocharger size in series configuration is higher than in parallel configuration, the breathing capability of the engine increases attaining higher EGR rates and lower exhaust manifold pressure. ~~Although due to turbo matching at low boost pressures, about 15% higher EGR rates are observed in a parallel configuration in comparison with series.~~ As the boost pressure increases higher EGR rates are achieved in series configuration along with lower turbine inlet pressure. The results for the same can be observed in Fig.7-(A),(C) and (E) for maximum EGR rates and Fig. 8 for exhaust manifold pressure.

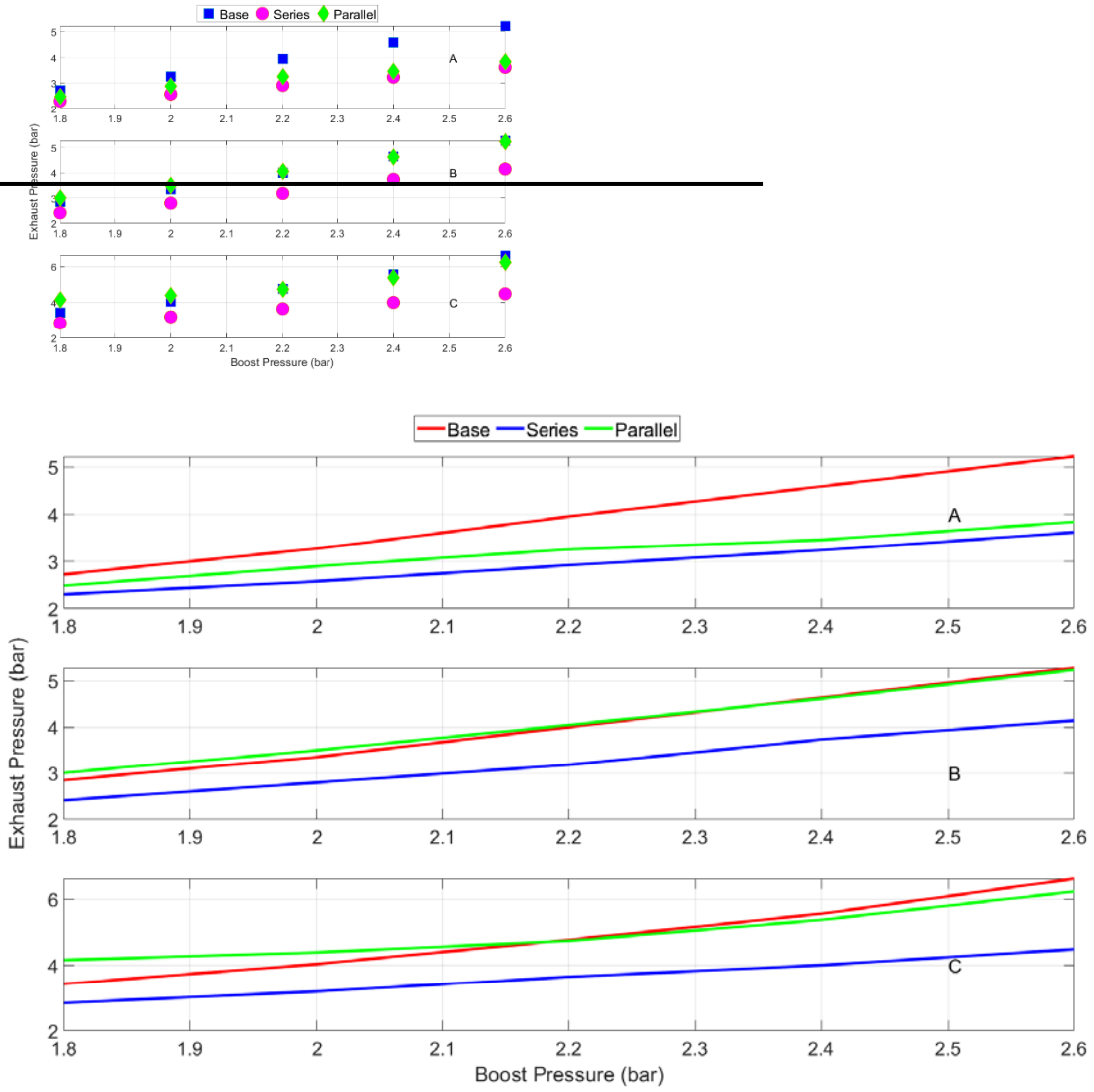

Figure 8: Exhaust manifold pressure (bar) Vs Exhaust Pressure (bar); A:1100 RPM; B:1500 RPM; C:2200 RPM

5.3 BSFC Assessment

To further assess the turbocharger configurations, in this section results on BSFC and pumping losses are analyzed for each configuration to attain 700 Nm of torque, while maintaining a constant air-to-fuel ratio of 18.

5.3.1 Partial load study at 1500 RPM

In Fig.9, information on EGR (%) is depicted in (A). (B) depicts the information on fuel consumption rate. (C) provides the data on exhaust pressure. (D) demonstrate pumping losses. All the information in Fig.9 is plotted against boost pressure. To attain a constant torque of 700 Nm higher EGR rates are possible when increasing the boost pressure. Trends in higher EGR rates can be observed in Fig.9(A) for all three configurations. Parallel configuration attains 2% higher EGR rate in comparison with the base configuration. These results are mostly consistent but at the highest boost pressure base architecture attains 0.5% higher EGR. This is because of elevated exhaust pressure, leading to higher pumping losses and thereby higher fuel consumption rate. Due to twin turbocharging higher EGR and lower fuel consumptions are observed in a parallel configuration in most of the engine running conditions. This is because of the increase in air density due to the twin compression of charge. The improvements in EGR rate and overall engine performance are higher in a series configuration. About 10% higher EGR is observed at low boost pressure and up to 5% enhanced EGR at higher boost pressure. ~~While comparing the results with the base configuration, parallel architecture results are similar in terms of EGR rate, BSFC, exhaust pressure, and pumping loss. While in series configuration, higher EGR rates are observed along with lower BSFC, exhaust pressure, and pumping loss.~~ Thanks to the design of the series architecture, as mentioned earlier, the exhaust gases are added in the intermediate stages between the two compressors. At this location, the charge pressure is higher than the ambient pressure. While in base and parallel architecture exhaust gases are supplied upstream of the compressor i.e., at ambient pressure. This expansion work done by the turbine at a constant turbine efficiency of 60% for all three speeds has caused an advantage for series configuration, to run with a nominal size turbine size and thereby enhanced performance using series configuration.

In parallel configuration, to attain higher boost pressures, as mentioned earlier due to turbo matching and to attain 60% turbine efficiency a small-sized turbocharger has been used. Along with a higher expansion ratio leading to higher turbine inlet pressure. And therefore, has a negative impact on pumping losses and higher BSFC. In series configuration since, the exhaust gases are supplied to the engine at the intermediate stage of compressors, both compressor, and turbine run with low compression and expansion ratio compared to parallel and base architecture. This resulted in low exhaust manifold pressure leading to lower pumping losses, resulting in an increase in the breathing capability of the engine. With an increase in a fresh charger and thereby high EGR rates along with low fuel consumption rate. On average, 5% of excess exhaust gases can be supplied using series configuration compared to single-stage turbo configuration and saving fuel consumption up to 11 g/kWh in average. While comparing results at each boost pressure, the benefits on BSFC when using series configuration increase when running with higher boost pressure, as depicted in Fig. 9(B).

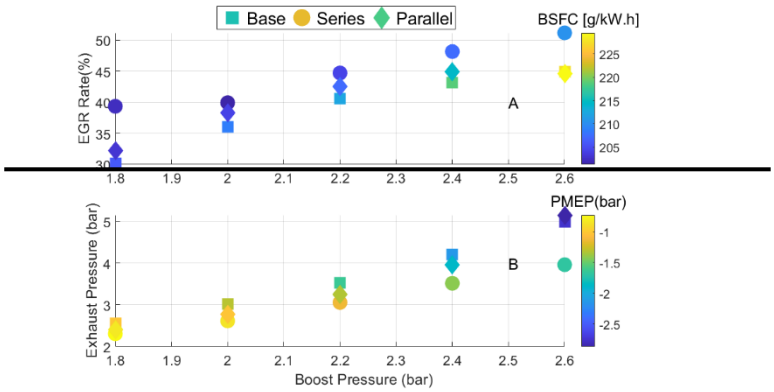

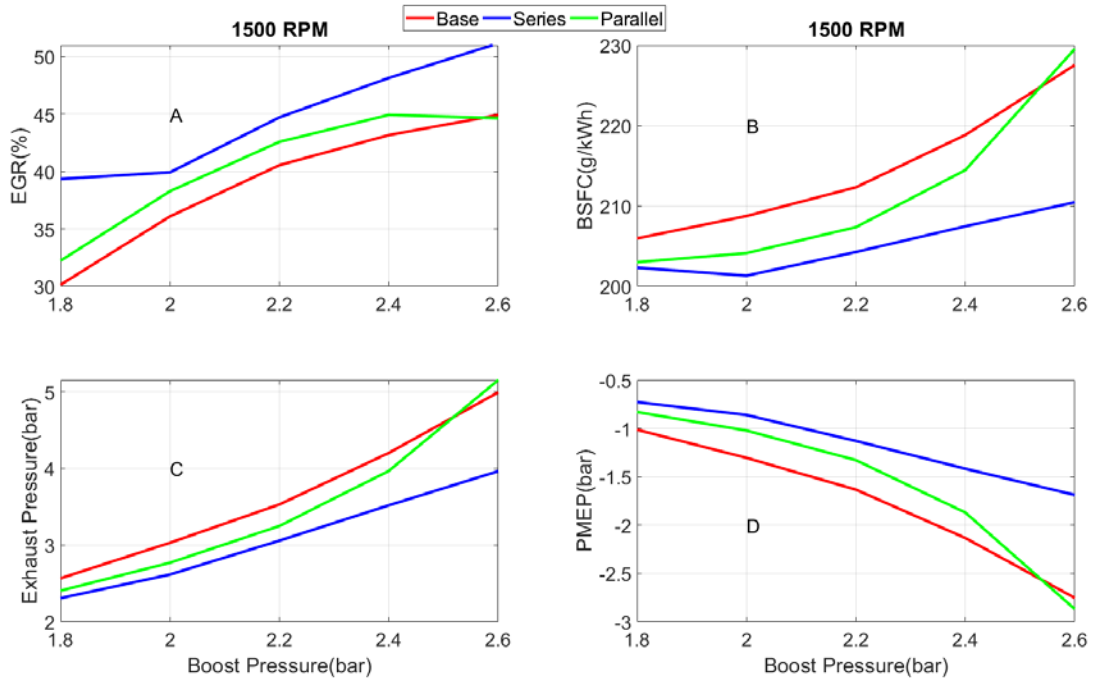

Figure 9: A: Boost pressure (bar) vs EGR (%); B: Boost pressure (bar) vs BSFC[g/kWh] ; C: Boost pressure (bar) vs Exhaust pressure (bar); D: Boost pressure (bar) vs PMEP (bar)

5.3.2 BSFC calculation at constant EGR rates

To finally assess the torque and fuel consumption figures that can be achieved with each configuration, simulations are conducted by fixing the EGR rate. These values are fixed from the assessment of the maximum EGR rate in section 5.2. A maximum of 40% EGR is fixed at 1100 and 1500 RPM and 30% at 2200 RPM. Results plotted with respect to boost pressure are demonstrated in Fig.10.

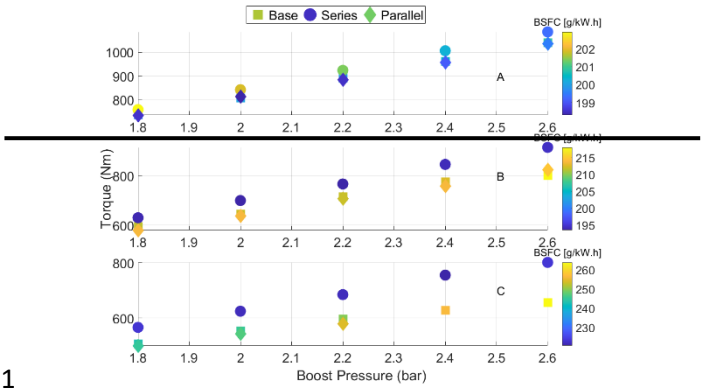

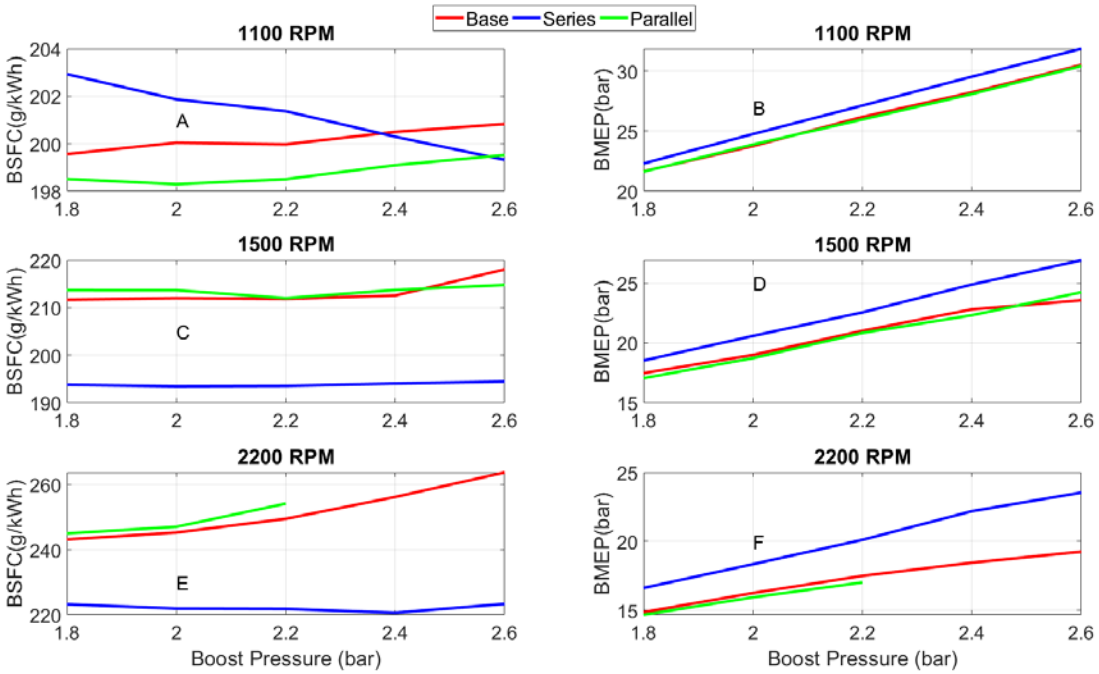

Figure 10: Boost pressure (bar) vs BSFC[g/kWh] A:1100 RPM;C:1500 RPM;E:2200 RPM; Boost pressure (bar) vs BMEP(bar) B:1100 RPM;D:1500 RPM;F:2200 RPM.

An important remark to include here is that parallel configuration at 2200 RPM and highest boost pressures exceeds the limit in the exhaust manifold pressure. Inspection of the results indicates that series configuration can attain higher BMEP at all three engine speeds. In series architecture, on an average 2 bar improved BMEP can be achieved at 1100 RPM while not being able to save any fuel due to turbo matching. At 1500 and 2200 RPM fuel consumption rate is decreased by an average of 20 g/kWh and 30 g/kWh, respectively. While able to attain 10% and 15% higher BMEP compared to the base configuration. This is because the series configuration employs a moderate-size turbocharger due to its engine layout.

5.4 Comparison with experimental results

From the above assessments of the trends and behavior of each boosting configuration, series architecture is used to compare results with experimental data using a single-stage turbocharger. As mentioned earlier, experiments are conducted on a single-stage turbocharger, and data from

these experiments are used as the boundary condition for this study. The experiment results are shown in Table 2.

From the above testing campaign, boost pressure is regulated by turbo matching and imposed AFR. EGR rates are regulated to attain desired torques, either by controlling the EGR valve in base configuration or by rack position of the turbine in stage-1 turbocharger of series architecture. This assessment is to evaluate the EGR rates and BSFC that can be attained using the EGR valve and twin-turbocharging. For a fair comparison, the size of the single-stage turbocharger and stage-2 turbocharger in series configuration is maintained the same. The size of the stage-1 turbocharger is optimized and maintained constant throughout the study and by adjusting for rack position to attain the engine torque values detailed in Table.1.

Table 2: Engine test Results

Engine speed	Boost pressure	Torque	Fuel	Air
RPM	bar	Nm	kg/h	kg/h
1100	1	200	5.7	210.8
1150	1.6	600	14.7	369
1200	3	1230	34.9	779.6
1450	1.1	127	5.04	301.1
1450	2	600	18.72	541.1
1450	3.1	1200	41.7	970.7
1500	2.1	600	19.8	585.1
2200	2.7	1080	56.8	1201.4

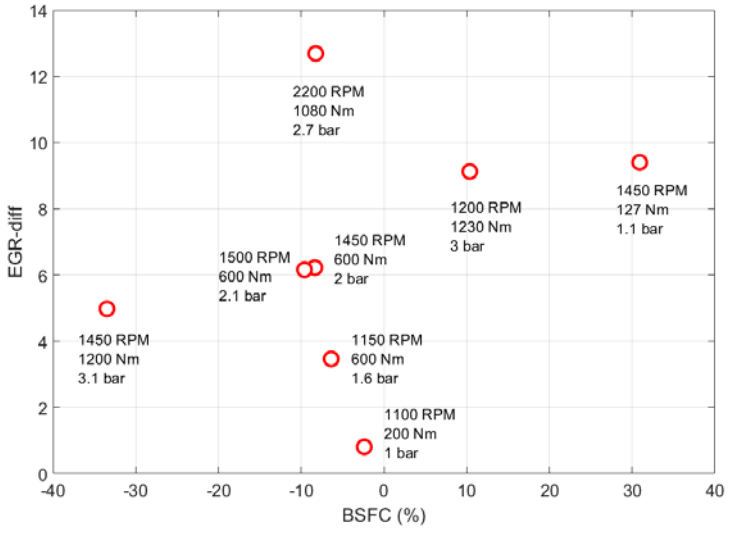

Figure 11: BSFC (%) vs EGR-diff

$$EGR - diff = EGR_{Series} - EGR_{base} \quad (5)$$

$$BSFC(\%) = \frac{BSFC_{series} - BSFC_{base}}{BSFC_{base}} (6)$$

Results are plotted in Fig. 11, which gives information on the BSFC and EGR differences as explained in Eq.5 and 6. From the above plot, it can be depicted that, at low engine speeds similar results in terms of EGR and BSFC can be observed, but as the engine speed increases the benefits from series configuration can be seen both in terms of higher EGR rates and BSFC. Negative BSFC implies fuel saving from series configuration over base configuration. It can be observed that at 1200 and 1450 RPM base configuration has better BSFC than the series configuration. But it should be considered the amount of EGR that the series configuration attains for the same operating point. It can be seen from Fig. 11, that series architecture always attains more EGR rates than base configuration. As exhaust gases inside the cylinder increase, the fuel consumption rate also increases- leading to higher BSFC. These are the outlier from all the 9 points assessed in this simulation. On average, comparing results with base configuration (excluding outlier point) series configuration attain 6% higher EGR rates and save up to 7% of fuel consumption rate compared to single-stage turbocharging.

6 Conclusions

~~A simulation-based assessment is carried out to evaluate the replacement of the EGR valve with a turbine and quantify the potential benefit of increased EGR rates along with better BSFC in an HD engine. For this analysis, a validated engine model using a single-stage turbocharger is used. Four different turbocharging layouts are developed, and two turbocharging configurations are discarded due to performance instabilities related to turbo-matching.~~

~~Clear advantages in increased EGR rates without fuel consumption penalty appear in twin-turbocharging architectures. Benefits become more relevant when the engine speed increases and when operating with higher intake manifold pressure values. Comparing the twin-turbocharging architectures, the series configuration attains higher EGR rates, along with performing far from the thermo-mechanical limit of the turbochargers.~~

~~At partial load operation, results show that parallel and base configurations work similarly in terms of EGR rates, BSFC, exhaust pressure, and pumping loss. While series configuration showed improved EGR and BSFC of up to 5% and 8% respectively, on average at all tested points.~~

~~The twin series configuration compared to experimental results using single-stage turbocharging reveals averaged values throughout the entire HD engine map of 6% points increase in EGR rate and save up to 7% in fuel consumption.~~

A simulation-based assessment is carried out to evaluate the replacement of the EGR valve with a turbine and quantify the potential benefit of increased EGR rates along with better BSFC in an HD engine. For this analysis, a validated engine model using a single-stage turbocharger is used. Four different turbocharging layouts are developed, and two turbocharging configurations are discarded due to performance instabilities related to turbo-matching.

Further assessments are performed on the series-2 and parallel configuration along with single-stage turbocharging configurations. The series of tests included maximum EGR study at full load, and engine operation at 1100, 1500, and 2200 RPM speeds. BSFC assessment in which layouts are

analyzed under two conditions: to attain 700Nm at 1500 RPM engine speed and constant EGR rates. The following conclusions are drawn from this assessment:

- Twin turbocharging has a higher performance to attain higher EGR and lower BSFC rates over single-stage turbocharging at higher engine speeds. On average in single-stage turbocharging configuration attain a maximum EGR rate of 50% at all three engine speeds. While results for Twin turbocharging show EGR rates higher than 50% can be attained.
- While comparing results for maximum EGR rate study for series and parallel architectures, parallel configuration performs similar to series configuration at 1100 RPM engine speed, that is providing minimal benefits. At higher engine speeds parallel configuration attains 5% higher EGR rates on average at low boost pressures compared to series architecture. But has the disadvantage of higher exhaust manifold pressure almost performing at the thermo-mechanical limit of 4.5 bar. At higher boost pressure series configuration attains higher EGR rates about 3% higher at 1500 RPM engine speed and about 10% higher EGR rates on average at 2200 RPM. Along with performing far from the thermo-mechanical limit of the turbochargers.
- In BSFC analysis to attain 700Nm, results show that parallel and base configurations work similarly in terms of EGR rates, BSFC, exhaust pressure, and pumping loss. The minimum EGR rate attained by parallel and base configuration is approximately 30% at 1.8 bar boost pressure, while for the same engine operation, series configuration attains 40% EGR rate having similar BSFC, Exhaust pressure, and pumping loss. At 2.6 bar boost pressure series configuration attain a maximum EGR rate of 50% with a BSFC value of 215 g/kWh. While base and parallel, configuration attains an EGR rate of 45% with BSFC of 225 g/kW.h and high pumping losses.

  BSFC calculation at fixed EGR rates, a very fever advantage of twin-turbocharging can be seen at 1100 RPM engine speed. As the engine speed increase, the potentiality of the series configuration can be observed. At 1500 RPM engine speed, series configuration has an average BSFC of 195 g/kWh approximately 9% lower than parallel and base configuration on average, while attaining higher torques. At 2200 RPM, parallel configuration reaches the thermo-mechanical limit of 4.5 bar in exhaust pressure at higher boost pressure. Comparing the results of series and base configuration show that on an average 100 Nm higher torques can be attained using series configuration while maintaining a low fuel consumption rate averaging 230 g/kWh.

From the above assessment, it can be concluded that the series configuration has better performance in terms of attaining higher EGR rates, low exhaust pressure, better fuel consumption rates, and lower pumping losses. This configuration is then compared with experimental results using single-stage turbocharging. The conclusions from this study are, on an average 6% higher EGR rates can be attained using series twin-turbocharging configurations and save up to 7% in fuel while comparing the results with single-stage turbocharging.

Acknowledgments

This research work has been supported by Grant PDC2021-120821-I00 funded by the Spanish Ministry of Science and Innovation (MCIN/AEI/10.13039/501100011033) and by the European Union NextGenerationEU/PRTR.

References

[1] Oldřich Vítek, Jan Macek, Miloš Polášek, Stefan Schmerbeck, and Thomas Kammerdiener, "Comparison of Different EGR Solutions," Apr. 2008, pp. 2008-01–0206. doi: 10.4271/2008-01-0206.

[2] Jong Heun Jun, Soon Ho Song, Kwang Min Chun, and Kyo Seung Lee, "Comparison of NOx level and BSFC for HPL EGR and LPL EGR system of heavy-duty diesel engine," Aug. 2007, pp. 2007-01–3451. doi: 10.4271/2007-01-3451.

[3] Masayuki Kobayashi *et al.*, "Effective BSFC and NOx Reduction on Super Clean Diesel of Heavy-Duty Diesel Engine by High Boosting and High EGR Rate," Apr. 2011, pp. 2011-01–0369. doi: 10.4271/2011-01-0369.

[4] Jose Galindo, Hector Climent, Benjamin Pla, and Chaitanya Patil, "EGR Transient Operations in Highly Dynamic Driving Cycles," *Int. J. Automot. Technol.*, vol. 21, no. 4, pp. 865–879, Aug. 2020, doi: 10.1007/s12239-020-0084-x.

[5] F. Millo, C. V. Ferraro, M. Gianoglio Bernardi, S. Barbero, and P. Pasero, "Experimental and Computational Analysis of Different EGR Systems for a Common Rail Passenger Car Diesel Engine," *SAE Int. J. Engines*, vol. 2, no. 1, pp. 527–538, Apr. 2009, doi: 10.4271/2009-01-0672.

[6] Robert C. Griffith, "Series Turbocharging for the Caterpillar Heavy-Duty On-Highway Truck Engines with ACERT^{TM} Technology," Apr. 2007, pp. 2007-01–1561. doi: 10.4271/2007-01-1561.

[7] Mohamed Shaaban Khalef, Alec Soba, and John Korsgren, "Study of EGR and Turbocharger Combinations and Their Influence on Diesel Engine's Efficiency and Emissions," Apr. 2016, pp. 2016-01–0676. doi: 10.4271/2016-01-0676.

[8] J. Galindo, J. R. Serrano, H. Climent, and O. Varnier, "Impact of two-stage turbocharging architectures on pumping losses of automotive engines based on an analytical model," *Energy Convers. Manag.*, vol. 51, no. 10, pp. 1958–1969, Oct. 2010, doi: 10.1016/j.enconman.2010.02.028.

[9] Jose´ Galindo, Hector Climent, Olivier Varnier, and Chaitanya Patil, "Effect of boosting system architecture and thermomechanical limits on diesel engine performance: Part II—transient operation," *Int. J Engine Res.*, vol. 19 (8), pp. 873–885, Aug. 2017.

[10] José Galindo, Hector Climent, Olivier Varnier, and Chaitanya Patil, "Effect of boosting system architecture and thermomechanical limits on diesel engine performance: Part-I—Steady-state operation," *Int. J. Engine Res.*, vol. 19, no. 8, pp. 854–872, Oct. 2018, doi: 10.1177/1468087417731654.

[11] F. Millo, F. Mallamo, and G. Ganio Mego, "The Potential of Dual Stage Turbocharging and Miller Cycle for HD Diesel Engines," Apr. 2005, pp. 2005-01–0221. doi: 10.4271/2005-01-0221.

[12] N. Dimitrakopoulos, G. Belgiorno, M. Tunér, P. Tunestål, and G. Di Blasio, "Effect of EGR routing on efficiency and emissions of a PPC engine," *Appl. Therm. Eng.*, vol. 152, pp. 742–750, Apr. 2019, doi: 10.1016/j.applthermaleng.2019.02.108.

[13] H. Zhang, L. Shi, K. Deng, S. Liu, and Z. Yang, “Experiment investigation on the performance and regulation rule of two-stage turbocharged diesel engine for various altitudes operation,” *Energy*, vol. 192, p. 116653, Feb. 2020, doi: 10.1016/j.energy.2019.116653.
[14] L. Leng, H. Qiu, X. Li, J. Zhong, L. Shi, and K. Deng, “Effects on the transient energy distribution of turbocharging mode switching for marine diesel engines,” *Energy*, vol. 249, p. 123746, Jun. 2022, doi: 10.1016/j.energy.2022.123746.
[15] C. Ke, K. Han, Y. Huang, X. Wang, and S. Bai, “Neural Network Based Nonlinear Model Predictive Control for Two-stage Turbocharged Diesel Engine Air-path System,” in *2021 33rd Chinese Control and Decision Conference (CCDC)*, May 2021, pp. 5770–5774. doi: 10.1109/CCDC52312.2021.9602515.
[16] Jan-Ola Olsson, Per Tunestål, Jonas Ulfvik, and Bengt Johansson, “The Effect of Cooled EGR on Emissions and Performance of a Turbocharged HCCI Engine,” Mar. 2003, pp. 2003-01–0743. doi: 10.4271/2003-01-0743.
[17] Dae Sik Kim and Chang Sik Lee, “Improved emission characteristics of HCCI engine by various premixed fuels and cooled EGR,” *Fuel*, vol. 85, no. 5, pp. 695–704, Mar. 2006, doi: 10.1016/j.fuel.2005.08.041.
[18] Malin Alriksson and Ingemar Denbratt, “Low Temperature Combustion in a Heavy Duty Diesel Engine Using High Levels of EGR,” Apr. 2006, pp. 2006-01–0075. doi: 10.4271/2006-01-0075.
[19] M. Elkelawy, E. A. El Shenawy, S. A. Mohamed, M. M. Elarabi, and H. Alm-Eldin Bastawissi, “Impacts of EGR on RCCI engines management: A comprehensive review,” *Energy Convers. Manag. X*, vol. 14, p. 100216, May 2022, doi: 10.1016/j.ecmx.2022.100216.
[20] M. Elkelawy, E. A. El Shenawy, S. A. Mohamed, M. M. Elarabi, and H. A.-E. Bastawissi, “Impacts of using EGR and different DI-fuels on RCCI engine emissions, performance, and combustion characteristics,” *Energy Convers. Manag. X*, vol. 15, p. 100236, Aug. 2022, doi: 10.1016/j.ecmx.2022.100236.
[21] Bang-Quan He, Shi-Jin Shuai, Jian-Xin Wang, and Hong He, “The effect of ethanol blended diesel fuels on emissions from a diesel engine,” *Atmos. Environ.*, vol. 37, no. 35, pp. 4965–4971, Nov. 2003, doi: 10.1016/j.atmosenv.2003.08.029.
[22] Mohamed Y. E Selim, “Effect of exhaust gas recirculation on some combustion characteristics of dual fuel engine,” *Energy Convers. Manag.*, vol. 44, no. 5, pp. 707–721, Mar. 2003, doi: 10.1016/S0196-8904(02)00083-3.
[23] J. Shin, J. Choi, J. Seo, and S. Park, “Pre-chamber combustion system for heavy-duty engines for operating dual fuel and diesel modes,” *Energy Convers. Manag.*, vol. 255, p. 115365, Mar. 2022, doi: 10.1016/j.enconman.2022.115365.
[24] D. T. Hountalas, G. C. Mavropoulos, and K. B. Binder, “Effect of exhaust gas recirculation (EGR) temperature for various EGR rates on heavy duty DI diesel engine performance and emissions,” *Energy*, vol. 33, no. 2, pp. 272–283, Feb. 2008, doi: 10.1016/j.energy.2007.07.002.
[25] Ayush Jain, Akhilendra Pratap Singh, and Avinash Kumar Agarwal, “Effect of split fuel injection and EGR on NOx and PM emission reduction in a low temperature combustion (LTC) mode diesel engine,” *Energy*, vol. 122, pp. 249–264, Mar. 2017, doi: 10.1016/j.energy.2017.01.050.
[26] N Ladommatos, S Abdelhalim, and H Zhao, “The effects of exhaust gas recirculation on diesel combustion and emissions,” *Int. J. Engine Res.*, vol. 1, no. 1, pp. 107–126, Feb. 2000, doi: 10.1243/1468087001545290.

[27] Takashi Suzuki, Akihiko Sato, and Koichi Suenaga, “Development of a Higher Boost Turbocharged Diesel Engine for Better Fuel Economy in Heavy Vehicles,” Feb. 1983, p. 830379. doi: 10.4271/830379.
[28] Changryul Choi, Sunhyuk Kwon, and Sunghwan Cho, “Development of Fuel Consumption of Passenger Diesel Engine with 2 Stage Turbocharger,” Apr. 2006, pp. 2006-01–0021. doi: 10.4271/2006-01-0021.
[29] Sylvain Saulnier and Stéphane Guilain, “Computational Study of Diesel Engine Downsizing Using Two-StageTurbocharging,” Mar. 2004, pp. 2004-01–0929. doi: 10.4271/2004-01-0929.
[30] Marc van Aken, Frank Willems, and Dirk-Jan de Jong, “Appliance of High EGR Rates With a Short and Long Route EGR System on a Heavy Duty Diesel Engine,” Apr. 2007, pp. 2007-01–0906. doi: 10.4271/2007-01-0906.
[31] M. Güven, H. Bedir, and G. Anlaş, “Optimization and application of Stirling engine for waste heat recovery from a heavy-duty truck engine,” *Energy Convers. Manag.*, vol. 180, pp. 411–424, Jan. 2019, doi: 10.1016/j.enconman.2018.10.096.
[32] R. Murali *et al.*, “A review on the correlation between exhaust backpressure and the performance of IC engine,” *J. Phys. Conf. Ser.*, vol. 2051, no. 1, p. 012044, Oct. 2021, doi: 10.1088/1742-6596/2051/1/012044.
[33] Z. Ma, Y. Gu, S. Zhu, M. Yang, and K. Deng, “Analysis on capability of power recovery of marine diesel engine at high backpressure conditions,” *Appl. Therm. Eng.*, vol. 204, p. 117933, Mar. 2022, doi: 10.1016/j.applthermaleng.2021.117933.
[34] T. M. Hao Dong and X. Phuong Nguyen, “EXHAUST GAS RECOVERY FROM MARINE DIESEL ENGINE IN ORDER TO REDUCE THE TOXIC EMISSION AND SAVE ENERGY: A MINI REVIEW,” *J. Mech. Eng. Res. Dev.*, vol. 42, no. 5, pp. 143–147, Aug. 2019, doi: 10.26480/jmerd.05.2019.143.147.
[35] V. P. and D. Deshmukh, “A comprehensive review of waste heat recovery from a diesel engine using organic rankine cycle,” *Energy Rep.*, vol. 7, pp. 3951–3970, Nov. 2021, doi: 10.1016/j.egyr.2021.06.081.
[36] V. V. Sinyavski, A. V. Krigulski, M. G. Shatrov, and L. N. Golubkov, “Estimation of Nitrogen Oxide Emission Reduction in a Boosted Truck Diesel Engine with Two-Stage Charging and Miller Cycle,” in *2021 Intelligent Technologies and Electronic Devices in Vehicle and Road Transport Complex (TIRVED)*, Nov. 2021, pp. 1–5. doi: 10.1109/TIRVED53476.2021.9639145.
[37] Anubhav, G. Nandan, and A. K. Shukla, “Analysis of Heat Energy Recovery from Lighter Automotive Vehicle,” in *2021 4th International Conference on Recent Developments in Control, Automation & Power Engineering (RDCAPE)*, Oct. 2021, pp. 90–94. doi: 10.1109/RDCAPE52977.2021.9633462.
[38] B. Orr, A. Akbarzadeh, M. Mochizuki, and R. Singh, “A review of car waste heat recovery systems utilising thermoelectric generators and heat pipes,” *Appl. Therm. Eng.*, vol. 101, pp. 490–495, May 2016, doi: 10.1016/j.applthermaleng.2015.10.081.
[39] P. Aranguren, D. Astrain, A. Rodríguez, and A. Martínez, “Experimental investigation of the applicability of a thermoelectric generator to recover waste heat from a combustion chamber,” *Appl. Energy*, vol. 152, pp. 121–130, Aug. 2015, doi: 10.1016/j.apenergy.2015.04.077.
[40] Y. Choi, A. Negash, and T. Y. Kim, “Waste heat recovery of diesel engine using porous medium-assisted thermoelectric generator equipped with customized thermoelectric modules,” *Energy Convers. Manag.*, vol. 197, p. 111902, Oct. 2019, doi: 10.1016/j.enconman.2019.111902.

[41] M. F. Remeli, L. Tan, A. Date, B. Singh, and A. Akbarzadeh, “Simultaneous power generation and heat recovery using a heat pipe assisted thermoelectric generator system,” *Energy Convers. Manag.*, vol. 91, pp. 110–119, Feb. 2015, doi: 10.1016/j.enconman.2014.12.001.
[42] José Galindo, Héctor Climent, Roberto Navarro, and Guillermo García-Olivas, “Assessment of the numerical and experimental methodology to predict EGR cylinder-to-cylinder dispersion and pollutant emissions,” *Int. J. Engine Res.*, Dec. 2020, doi: 10.1177/1468087420972544.
[43] Jose Serrano, Hector Climent, Roberto Navarro, and David González-Domínguez, “Methodology to Standardize and Improve the Calibration Process of a 1D Model of a GTDI Engine,” Apr. 2020, pp. 2020-01–1008. doi: 10.4271/2020-01-1008.